



This is an author produced version of *Enhanced Southern Ocean marine productivity due to fertilization by giant icebergs*.

White Rose Research Online URL for this paper:  
<http://eprints.whiterose.ac.uk/96582/>

---

**Article:**

Duprat, L.P.A.M., Bigg, G.R. and Wilton, D.J. (2016) Enhanced Southern Ocean marine productivity due to fertilization by giant icebergs. *Nature Geoscience*, 9 (3). pp. 219-221. ISSN 1752-0894

<http://dx.doi.org/10.1038/ngeo2633>

---

## **Enhanced Southern Ocean marine productivity from fertilization by giant icebergs**

**Luis P. A. M. Duprat, Grant R. Bigg\* and David J. Wilton**

**Department of Geography, University of Sheffield, Sheffield S10 2TN, U. K.**

**Primary productivity has been shown to be enhanced within a few kilometres of icebergs in the Weddell Sea<sup>1,2</sup> due to the input of terrigenous nutrients and trace elements during melting. However, few studies in the Southern Ocean have investigated the influence of giant icebergs (those > 18 km in length) on marine primary production<sup>1,3</sup>. Here we present an assessment of this productivity using ocean colour data from 175 images, associated with 17 giant icebergs in the open ocean over the period 2003-2013. Our findings suggest the fertilizing influence of individual giant icebergs typically extends over a radius of at least 4-10 times their length, more than an order of magnitude larger area than found in previous studies restricted to sub-kilometre scale icebergs<sup>2</sup> or limited by ship-based surveys<sup>1</sup>. This suggests that up to a fifth of the Southern Ocean's downward carbon flux originates with giant iceberg fertilization. Given the likely increase in giant iceberg calving this century, if the West Antarctic Ice Sheet has indeed passed its stable point<sup>4</sup>, this negative feedback on the carbon cycle may increase.**

The Southern Ocean is a significant sink in the ocean component of the global carbon cycle, contributing ~ 10% of the ocean's total carbon sequestration through a mixture of chemical and biologically-driven processes<sup>5</sup>. However, its contribution is

at a lower level than that of the smaller South Pacific and Indian Oceans<sup>5</sup>, due to its low concentration of dissolved iron, an important trace nutrient for primary production<sup>6</sup>. Atmospheric dust is a major background source of iron to the region<sup>7</sup>, but iron-rich sediment fluxes from islands<sup>8</sup>, continental shelves<sup>9</sup>, ice sheet meltwater<sup>10</sup> and melting icebergs<sup>1</sup> are known to be other, locally much more important, sources of iron. There are a few large-scale estimates of the contribution of icebergs to the Southern Ocean iron flux, derived from modelling studies of typical sub-kilometre sized icebergs<sup>11, 12</sup>, scaling up of observational studies<sup>13, 14</sup> or remote sensing studies<sup>2</sup>. However, these assume iceberg inputs are well represented by those from the smaller, sub-kilometre, peak in the very bimodal size distribution<sup>15</sup>. In fact about half the total iceberg discharge volume is made up of giant icebergs<sup>15</sup> - those exceeding 18 km in horizontal dimension - and there have currently only been two observational studies of the phytoplankton blooms close to individual giant icebergs, both in conditions within or near sea-ice cover in the Weddell Sea<sup>1, 3</sup>. Such areas may be subject to enhanced productivity due to the impact of sea-ice fertilization<sup>16</sup>. While the calving of giant icebergs is very episodic<sup>15</sup>, they derive from a range of geographical and geological environments around Antarctica, and thus likely have different iron and nutrient characteristics. Several dozen such icebergs are present in the Southern Ocean at any one time<sup>15</sup>, and they can survive for many years. Even when in areas of open water giant icebergs can survive for longer than a year<sup>17</sup>. Here we examine the chlorophyll signature from a range of giant icebergs in the open Southern Ocean using remote sensing, to show that ocean fertilization from such icebergs is much larger than previously suspected.

Chlorophyll levels are well known to be raised near icebergs<sup>1, 2, 18</sup>. This derives from the meltwater plumes from icebergs containing significant concentrations of iron, but

also a range of other nutrients<sup>14</sup>. As the Southern Ocean is a High Nutrient Low Chlorophyll (HNLC) region<sup>6</sup>, it is the bioavailable iron known to be in nanoparticle aggregates of ferrihydrite and goethite in iceberg sediments<sup>13</sup> that is the key nutrient within this meltwater. Dissolution of these particles leads to enriched concentrations of dissolved iron in the meltwater plume at levels 10-1000 times those due to atmospheric dust<sup>19</sup>. Ship-based studies have demonstrated that, for an iceberg of maximum horizontal size  $L_i$ , chlorophyll levels are enhanced downstream over a distance of  $\sim L_i$ <sup>20</sup>. Similarly, it has been shown using SeaWiFS ocean colour that the probability of chlorophyll being enhanced 6 days after an iceberg with a  $L_i$  of  $\sim 1$  km has passed over a location is a third higher than from chance alone<sup>2</sup>. However, the inherent practical limitations of these studies mean that an accurate picture of the chlorophyll enhancement in waters surrounding a giant iceberg is not known.

The potential for major enhanced production around giant icebergs is shown in Figure 1, where chlorophyll levels in excess of 10 times background extend in plumes at least  $3-4L_i$  both upstream and downstream of iceberg C16. Examining the chlorophyll signal of a range of giant icebergs calved from around Antarctica over a 10 year period (see Methods and Supplementary Table 1) it is found that such an enhancement is ubiquitous and long-lasting. A chlorophyll enhancement of a factor of 10 is found at least a month following passage of a giant iceberg (Figure 2a). This order of magnitude enhancement peaks 50-200 km from the giant iceberg, but some enhancement typically extends for over 500 km from the berg (Figure 2b), and occasionally for over 1000 km. Note that Figure 2b also implies that measurements taken near a giant iceberg, as has normally been necessary in field campaigns, will significantly underestimate the fertilization peak. This lower production near the iceberg, and the unexpected enhancement of production ahead of the iceberg, are

likely due to the buoyant plume associated with the basal melting of the iceberg. The buoyant meltwater plume takes a little time to rise to the surface ahead of the iceberg<sup>20</sup>. This displacement, coupled with the need for time for the enhanced production to develop and possible increased phytoplankton predation close to the iceberg<sup>20</sup>, means that the fertilization near the iceberg is lower than further afield. It then spreads out near the surface, transporting dissolved material, allowing this fertilizing material to move ahead of the iceberg driven by the surface ocean current. Figure 1 shows that this forward fertilization can be substantial.

There is no statistically significant difference between the magnitude of fertilization effects in spring and summer. Similarly, there is no statistically significant difference between the origins of giant icebergs in their fertilization effect a month after passage (Figure 2c). However, while there is a large degree of variability in the short-term fertilization effect of giant icebergs from sector D of the Antarctic (0-90°E), giant bergs from sectors B and C (90-180°W and 90-180°E respectively) have only half the impact of those from sector A (0-90°W). These differences correlate very well with the large-scale geology of Antarctica. Almost all of coastal East Antarctica (sectors C and D) is composed of PreCambrian high grade metamorphic rock from granitic facies<sup>21</sup>, which will be less easily weathered than the low grade Mesozoic metasedimentary and metavolcanic rocks of the Antarctica Peninsula (from which most of the sector A icebergs derive<sup>15</sup>). The exception to the East Antarctic geology is that the metamorphic grade of rock lowers poleward into the Amery Basin (~70°E)<sup>20</sup>, a major source of giant icebergs from sector D, consistent with a range of levels of ice-rafted debris embedded within sector D's icebergs. It is also worth noting that giant icebergs from sectors B and C often travel further before reaching the open sea<sup>15</sup>, and thus being only then able to be more easily examined by ocean

colour instruments, meaning that their sediment load is likely to be depleted before they reach open water.

Noting these major increases in estimated productivity due to giant icebergs, it is pertinent to examine their implications for estimates of the contribution of icebergs in the Southern Ocean to global biogeochemical cycles. Firstly, it is known that there is indeed an increase in the net flux of carbon to the sea floor near icebergs. A study of carbon export using Lagrangian Sediment Traps<sup>18</sup> showed a net carbon export past 600 m depth of  $5.6 \text{ mg m}^{-2} \text{ day}^{-1}$  within 30 km of iceberg C18a, compared to a background of  $2.5 \text{ mg m}^{-2} \text{ day}^{-1}$ . Given that the peak enhancement distance from our analysis (Figure 2b) is at 100 km, but the Traps used in the ship survey<sup>18</sup> were within 30 km of C18a, the estimate above of  $5.6 \text{ mg m}^{-2} \text{ day}^{-1}$  is likely to be an underestimate of the peak flux. However, it gives us a starting point for a conservative global calculation of the iceberg contribution to the carbon cycle.

There have been two full biogeochemical model simulations of the impact of iceberg melting on production in the Southern Ocean<sup>9, 11</sup>. Both suggest that coastal sediment fluxes are the major sources of iron fertilization in the Southern Ocean, leading to up to 75% of the total productivity. Both also have ~ 10% of the productivity deriving from icebergs. However, they were required to make assumptions about the mean bioavailable iron, only including dissolved iron and neglecting the nanoparticulate iron attached to sediments<sup>13</sup>, and that this is spread evenly according to model estimates of meltwater flux<sup>15</sup>. Given our study's implications of an area of influence for giant icebergs of more than an order of magnitude above that of "typical" icebergs, and that approximately half of the iceberg discharge is as giant icebergs<sup>15</sup>, with several dozen giant icebergs present in the Southern Ocean at any one time<sup>4</sup>, these model calculations of iceberg productivity are likely to be a significant

underestimate. This conclusion is supported by another modelling study which concentrated on glacial meltwater and higher iceberg fluxes, but did not include shelf sediment iron fluxes<sup>12</sup>.

A rough estimate of this giant iceberg carbon export is 0.012-0.040 Gt yr<sup>-1</sup> (see Methods), approaching 10-20% of the estimated Southern Ocean total carbon export<sup>5</sup>. Our analysis therefore suggests that the total impact of icebergs on the carbon cycle in the Southern Ocean has been under-estimated, and may constitute up to a fifth of the total carbon export of that ocean.

While it is difficult to discern net trends over time in the very episodic calving of giant icebergs<sup>15</sup>, satellite gravity measurements suggest that there has been a 5% increase in ice discharge from Antarctica over the last two decades<sup>22</sup>. Recently, concern over the stability of the West Antarctic Ice Sheet has arisen<sup>4, 23</sup>, with implications for more ice discharge in the future and thus carbon drawdown through fertilization. Note that even an increase in regional sediment-rich ice sheet meltwater into coastal waters can lead to enhanced fertilization<sup>10, 12, 24</sup>, although that associated with giant iceberg melting may be even greater (Figure 3). The future may therefore see an increase in Southern Ocean carbon sequestration through this iceberg fertilization mechanism, acting as a secondary negative feedback on climate change.

## **Methods**

The giant iceberg tracks used for the main analysis come from the Brigham Young University Center for Remote Sensing Iceberg Tracking database ([www.scp.byu.edu/data/iceberg/database1.html](http://www.scp.byu.edu/data/iceberg/database1.html)) which uses satellite scatterometer

backscatter to identify giant icebergs<sup>26</sup>. The resolution achievable by these satellite sensors is 4-5 km<sup>26</sup>, but only those icebergs meeting the giant iceberg definition of having an  $L_i > 18$  km enter the database from which we selected the icebergs to be analysed. All icebergs examined are therefore well resolved.

Once the positions of giant icebergs were obtained, the Level 1 and 2 MODIS ocean colour images were exported from [oceancolor.gsfc.nasa.gov](http://oceancolor.gsfc.nasa.gov) using SeaDAS software v7.0.2. Chlorophyll concentrations were analysed from eleven years (2003-2013) for 65 positions during a one-month period 20 days prior to a giant iceberg passage, 63 positions for the seven-day period post-passage, and 47 values for the seven-day period following the iceberg passage. These came from 17 giant iceberg tracks (see Supplementary Table S1). The number of positions for icebergs from the A-D sectors were 22, 16, 15 and 10 respectively. The positions were taken from sea-ice free areas, restricting the number of possible images analysed from sectors B-D, and were almost all from equatorward of 60°S. Only portions of tracks were chosen where it was clear that the icebergs were not grounded, as can be seen from the sequence of positions in Supplementary Table S1. Note also that the one iceberg, C19a, which was followed both before and after austral winter (2008) remained in open water throughout the entire time between its first and last used image<sup>27</sup>. The mean chlorophyll concentration was obtained from a 15 km radius centred on the iceberg's geographical coordinates using the geometry mask tool from the SeaDAS software. The significant time difference between the before and after passage values was used because of the presence of major plumes both upstream and downstream from a giant iceberg's position (Figure 1).

A selection of 20 images (Supplementary Table S2 and Supplementary Methods) where a clear and delimited plume of increased chlorophyll could be visually



associated with the iceberg was chosen to draw a chlorophyll concentration profile with respect to distance from the iceberg (Figure 2b). A random line was drawn from the iceberg border towards the background value outside the plume, crossing the plume along its longest axis.

There are clear limitations to the study. The number of images obtained were restricted due to the high degree of cloudiness of the Southern Ocean, and the limited number of sun-lit months further south. A number of the images are likely to be affected by other iron sources, such as coastal sediment fluxes from South Georgia<sup>28, 29</sup>, although this was minimized as much as possible. Another limitation is that MODIS tends to overestimate chlorophyll concentrations that are low, minimizing the impact found. However, overall, MODIS's error accuracy for surface layer measurements in depths > 20 m is close to the instrument 35% target error<sup>30</sup>. A final limitation is that deep chlorophyll concentrations may occasionally be disturbed by passage of an iceberg, leading to an artificially enhanced chlorophyll level<sup>2</sup>.

To estimate the additional carbon export through the increased area of influence of giant icebergs found in this study the following calculations were made. The observed  $2.5 \text{ mg m}^{-2} \text{ day}^{-1}$  background export<sup>18</sup> was assumed to relate to the far-field chlorophyll concentration of Figure 2b. From Figure 2, this was assumed to be increased to  $25 \text{ mg m}^{-2} \text{ day}^{-1}$  over an area of  $\pi(4L_i)^2$ , or  $12.5 \text{ mg m}^{-2} \text{ day}^{-1}$  over an area of  $\pi(10L_i)^2$  where a typical giant iceberg  $L_i \sim 30 \text{ km}$ , and there are typical 30 such icebergs in the Southern Ocean<sup>15, 26</sup>. This gives a total giant iceberg export of  $0.012\text{-}0.040 \text{ Gt yr}^{-1}$ .

The images from Figure 3 were obtained from analyses and visualizations produced with the Giovanni online data system, developed and maintained by NASA GES

DISC ([gdata1.sci.gsfc.nasa.gov/daac-bin/G3/gui.cgi?instance\\_id=ocean\\_month](http://gdata1.sci.gsfc.nasa.gov/daac-bin/G3/gui.cgi?instance_id=ocean_month)).

The track of iceberg B31 in Figure 3 comes from using a range of sources over January-March 2014: Terra and Aqua satellite MODIS reflectance, available from [earthdata.nasa.gov/labs/worldview](http://earthdata.nasa.gov/labs/worldview) ; and SAR data from the TerraSAR-X and Radarsat2 satellites.

## References

1. Smith Jr., K. L., Robison, B. H., Helly, J. J. *et al.* Free-drifting icebergs: hot spots of chemical and biological enrichment in the Weddell Sea. *Science*, **317**, 478-482 (2007).
2. Schwarz, J. N. & Schodlok, M. P. Impact of drifting icebergs on surface phytoplankton biomass in the Southern Ocean: ocean colour remote sensing and in situ iceberg tracking. *Deep-Sea Res. I*, **56**, 1727-1741 (2009).
3. Helly, J. J., Kaufmann, R. S., Stephenson, G. R. & Vernet, M. Cooling, dilution and mixing of ocean water by free-drifting icebergs in the Weddell Sea. *Deep-Sea Res. II*, **58**, 1336-1345 (2011).
4. Joughin, I., Smith, B. E. & Medley, B. Marine ice sheet collapse potentially under way for the Thwaites Glacier Basin, West Antarctica. *Science*, **344**, 735-738 (2014).
5. Ciais, P., Sabine, C., Bala, G. *et al.* Carbon and Other Biogeochemical Cycles. In: *Climate Change 2013: The Physical Science Basis. Contribution of Working Group I to the Fifth Assessment Report of the Intergovernmental Panel on Climate Change* (Stocker, T. F., Qin, D., Plattner, G.-K. *et al.* (eds.)). Cambridge University Press, Cambridge, United Kingdom and New York, NY, USA, p. 465-570 (2013).

6. Martin, J. H., Fitzwater, S. E. & Gordon, R. M. Iron deficiency limits phytoplankton growth in Antarctic waters. *Glob. Biogeochem. Cyc.*, **4**, 5-12 (1990).
7. Mahowald, N. M., Engelstaedter, S., Luo, C. *et al.* Atmospheric iron deposition: global distribution, variability and human perturbations. *Ann. Rev. Mar. Sci.*, **1**, 245-278 (2009).
8. Blain, S., Treguer, P., Belviso, S. *et al.* A biogeochemical study of the island mass effect in the context of the iron hypothesis: Kerguelen Islands, Southern Ocean. *Deep-Sea Res. I*, **48**, 163-187 (2001).
9. Lancelot, C., de Montety, A., Goosse, H. *et al.* Spatial distribution of the iron supply to phytoplankton in the Southern Ocean: a model study. *Biogeosci.*, **6**, 2861-2878 (2009).
10. Hawkings, J. R., Wadham, J. L., Tranter, M. *et al.* Ice sheets as a significant source of highly reactive nanoparticulate iron to the oceans. *Nature Comm.*, **5**, doi: 10.1038/ncomms4929 (2014).
11. Wadley, M. R., Jickells, T. D. & Heywood, K. J. The role of iron sources and transport for Southern Ocean productivity. *Deep-Sea Res. I*, **87**, 82-94 (2014).
12. Death, R., Wadham, J. L., Monteiro, F. *et al.* Antarctic ice sheet fertilises the Southern Ocean. *Biogeosci.*, **11**, 2635-2643 (2014).
13. Raiswell, R., Benning, L. G., Tranter, M. & Tulaczyk, S. Bioavailable iron in the Southern Ocean: the significance of the iceberg conveyor belt. *Geochem. Trans.*, **9**, doi: 10.1186/1467-4866-9-7 (2008).
14. Wadham, J. L., De'ath, R., Monteiro, F. M. *et al.* The potential role of the Antarctic Ice Sheet in global biogeochemical cycles. *Earth Env. Sci. Trans. Roy. Soc. Edinburgh*, **104**, 55-67 (2013).

15. Silva, T. A. M., Bigg, G. R. & Nicholls, K. W. The contribution of giant icebergs to the Southern Ocean freshwater flux. *J. Geophys. Res. Oceans*, **111**, C03004 (2006).
16. Lannuzel, D., Schoemann, V., de Jong, J. *et al.* Iron study during a time series in the western Weddell pack ice. *Mar. Chem.*, **108**, 85-95 (2008).
17. Jansen, D., Schodlok, M. & Rack, W. Basal melting of A-38B: a physical model constrained by satellite observations. *Rem. Sens. Env.*, **111**, 195-203 (2007).
18. Smith Jr., K. L., Sherman, A. D., Shaw, T. J. *et al.* Carbon export associated with free-drifting icebergs in the Southern Ocean. *Deep-Sea Res. II*, **58**, 1485-1496 (2011).
19. Shaw, T. J., Raiswell, R., Hexel, C. R. *et al.* Input, composition and potential impact of terrigenous material from free-drifting icebergs. *Deep-Sea Res. II*, **58**, 1376-1383 (2011).
20. Smith Jr., K. L., Sherman, A. D., Shaw, T. J. *et al.* Icebergs as unique Lagrangian ecosystems in polar seas. *Ann. Rev. Mar. Sci.*, **5**, 269-287 (2013).
21. AGS, *Tectonic Map of Antarctica*, Antarctic Map Folio Series, Folio 12-Geology, Amer. Geogr. Soc. (1970).
22. Rignot, E., Velicogna, I., van den Broecke, M. R. *et al.* Acceleration of the contribution of the Greenland and Antarctic ice sheets to sea level rise. *Geophys. Res. Lett.*, **38**, L05503, (2011).
23. Paolo, F. S., Fricker, H. A. & Padman, L. Volume loss from Antarctic ice shelves is accelerating. *Science*, **348**, 327-331 (2015).
24. Staham, P. J., Skidmore, M. & Tranter, M. Inputs of glacially derived dissolved and colloidal iron to the coastal ocean and implications for primary productivity. *Glob. Biogeochem. Cycles*, **22**, GB3013 (2008).

25. Bigg, G. R., Marsh, R. A., Wilton, D. J. & Ivchenko, V. B31 – a giant iceberg in the Southern Ocean, *Ocean Challenge*, **20**, 32-34 (2014).
26. Stuart, K. M. & Long, D. G. Tracking large tabular icebergs using the SeaWinds Ku-band microwave scatterometer, *Deep-Sea Res. II*, **58**, 1285-1300 (2011).
27. Matsumoto, H., Bohnenstiehl, D. R., Tournadre, J. *et al.* Antarctic icebergs: a significant natural ocean sound source in the Southern Hemisphere. *Geochem. Geophys. Geosys.*, **15**, 3448-3458 (2014).
28. Korb, R. E., Whitehouse, M. J., Gordon, M. *et al.* Summer microplankton community structure across the Scotia Sea: implications for carbon export. *Biogeosci.*, **7**, 343-356 (2010).
29. Borrione I. & Schlitzer, R. Distribution and recurrence of phytoplankton blooms around South Georgia, Southern Ocean. *Biogeosci.*, **10**, 217-231 (2013).
30. Bierman, P., Lewis, M., Ostendorf, B. *et al.* A review of methods for analysing spatial and temporal patterns in coastal water quality. *Ecological Indic.*, **11**, 103-114 (2011).

**\* Corresponding Author, to whom correspondence and requests for materials should be addressed:** Grant R. Bigg, Department of Geography, University of Sheffield, Winter Street, Sheffield S10 2TN, U. K. e-mail: grant.bigg@sheffield.ac.uk

### **Acknowledgements**

Much of this work followed from the MSc dissertation of LPAMD. We also acknowledge support for part of the work from the Natural Environment Research Council Urgency Grant NE/L010054/1, "Tracking and prediction of the giant Pine Island iceberg", and SAR images from the German Aerospace Center Projects OCE2116 and 2184 and the European Space Agency project 16456. We wish to

thank the Canadian Space Agency for providing the data from the latter ESA project. We also wish to thank Elivane Victor, who helped LPAMD with some of the statistics, and Julia Thompson, whose MSc research brought the comparisons shown in Figure 3 to our attention.

### **Author Contributions**

GRB and LPAMD conceived the project; LPAMD carried out much of the analysis and assisted with writing; GRB contributed to the analysis and was the principal writer of the final manuscript. DJW carried out some of the tracking work shown in Figure 3, and commented on the manuscript.

### **Competing financial interests**

The authors declare no competing financial interests.

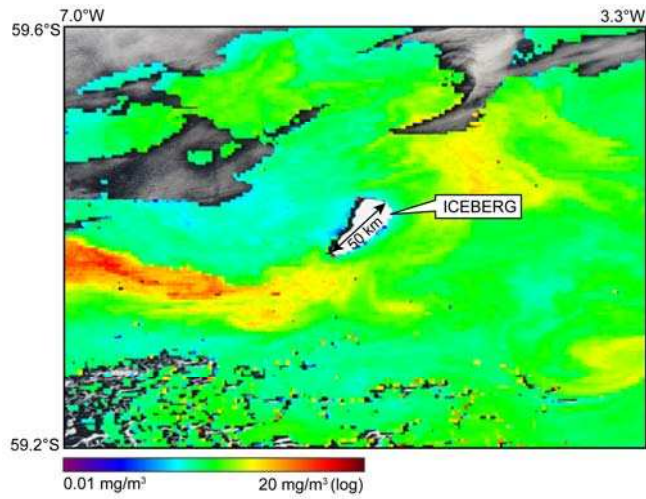


**Figure 1 | Chlorophyll-a concentration on 12 January 2013, from MODIS Aqua satellite.** Giant iceberg C16 is visible in the centre of the picture, with enhanced levels spreading SW and NE from the iceberg. Greyscale areas show cloud cover.

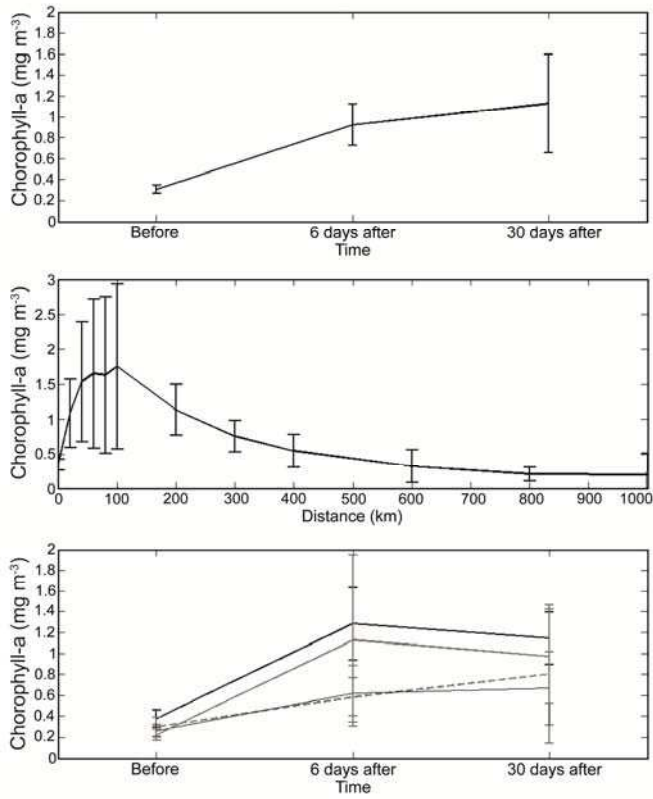


**Figure 2 | Mean chlorophyll level associated with the passage of a giant**

**iceberg.** a) Mean chlorophyll level before and after passage; b) at a distance from such an iceberg; and c) sector dependence of mean chlorophyll before and after passage (A: ---; B: - - -; C: ---; D: ---). The levels are in  $\text{mgm}^{-3}$  and 95% confidence intervals are shown.



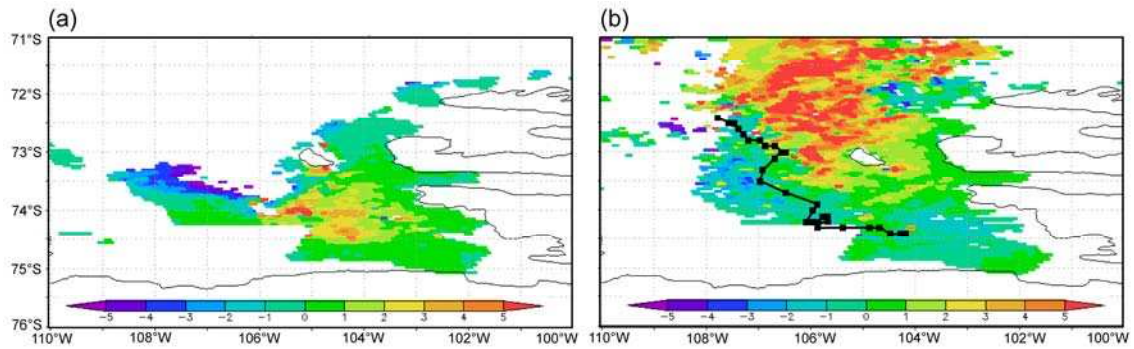


**Figure 3 | Chlorophyll concentration anomaly in the Pine Island Bay region of West Antarctica related to passage of giant iceberg, B31.** Means for Jan-Mar of a) 2011 and b) 2014, from the MODIS Aqua satellite. The units are in  $\text{mg m}^{-3}$ , relative to the Jan-Mar mean over 2003-15. Note the increased productivity offshore in 2014, downstream of B31<sup>25</sup>. The path of B31 over those 3 months is shown by the black line in b). White areas over the sea were covered by cloud for most of the respective 3 months.